

Low mass dilepton production in pp, p–Pb and Pb–Pb collisions with ALICE

Alessandro De Falco^{1,a} for the ALICE Collaboration

¹ *Università di Cagliari and INFN Sezione di Cagliari*

Abstract. Low mass vector meson (ρ , ω , ϕ) production provides key information on the hot and dense state of strongly interacting matter produced in high-energy heavy-ion collisions (called Quark-Gluon Plasma, QGP). Strangeness enhancement is one of the possible signatures of the Quark-Gluon Plasma formation and can be accessed through the measurement of ϕ meson production with respect to ρ and ω mesons. The production dynamics and hadronization process in relativistic heavy-ion collisions can be probed through the measurement of the ϕ nuclear modification factor.

We present results on the low mass dimuon analysis in pp, p–Pb and Pb–Pb collisions. In pp collisions at $\sqrt{s} = 2.76$ TeV the ϕ differential cross section as a function of the transverse momentum has been measured, serving as a baseline for Pb–Pb data.

The ϕ yield and the nuclear modification factor R_{pPb} at forward and backward rapidity have been measured for p–Pb collisions at $\sqrt{s} = 5.02$ TeV. At forward rapidity, R_{pPb} increases as a function of p_T , saturating for $p_T > 3$ GeV/c at $R_{pPb} \sim 1$. At backward rapidity, R_{pPb} shows an increase as a function of the transverse momentum up to a factor of 1.6 for $p_T \sim 3$ –4 GeV/c, followed by a decrease at higher p_T .

The ϕ yield and nuclear modification factor R_{AA} have been measured for Pb–Pb collisions at $\sqrt{s_{NN}} = 2.76$ TeV in the intermediate p_T region $2 < p_T < 5$ GeV/c, as a function of the number of participating nucleons. Remarkable differences are observed in the comparison between the results at forward rapidity in the dimuon channel and the ones measured in the same p_T range at midrapidity in the hadronic channel $\phi \rightarrow KK$.

In the dielectron channel at midrapidity, the invariant mass distributions in the range $0 < m_{ee} < 3$ GeV/c² are compared with the expected hadronic sources for pp collisions at $\sqrt{s} = 7$ TeV, and for p–Pb collisions at $\sqrt{s_{NN}} = 5.02$ TeV. Latest results of the analysis of Pb–Pb collisions at $\sqrt{s_{NN}} = 2.76$ TeV are presented.

1 Introduction

Low mass vector meson (ρ , ω , ϕ) production provides key information on the hot and dense state of strongly interacting matter produced in high-energy heavy-ion collisions. In particular, strangeness production can be accessed through the measurement of ϕ meson production, while the measurement of the ρ spectral function can be used to reveal in-medium modifications of hadron properties close to the QCD phase boundary. At low transverse momenta, $p_T < 2$ GeV/c, hadron production is governed by soft processes which can be described in terms of hydrodynamical and thermal models [1, 2],

^ae-mail: alessandro.de.falco@ca.infn.it

while at high p_T ($p_T > 5$ GeV/ c) hard processes dominate. In the latter region, yields are suppressed due to the parton energy loss caused by collisions and gluon bremsstrahlung [3]. At intermediate p_T ($2 < p_T < 5$ GeV/ c), light mesons are suppressed with respect to binary scaling, differently from protons and antiprotons [4]. In this context, it is interesting to compare their suppression pattern with the one of the ϕ , which is a meson having a mass similar to the proton one.

The detection of the ϕ meson through its decay in lepton pairs has the advantage that, differently from the K^+K^- channel, dileptons are not influenced by final state interactions, like rescattering and absorption, which may affect the ϕ reconstructed via the KK decay at low p_T [5].

Vector meson production in pp collisions provides a reference for the determination of the nuclear modification factor (see Equation 1 below). Moreover, it is interesting by itself, since it can be used to tune particle production models in the LHC energy range.

In order to disentangle cold nuclear matter (CNM) effects from the ones due to the hot and dense medium, data acquired in p–Pb collisions are necessary, since in this system no QGP is expected to be formed.

The ALICE experiment at the LHC can access low-mass dileptons both at forward rapidity, in the dimuon channel, and at midrapidity in the dielectron channel. The focus of this contribution will be on vector meson production in the dimuon channel. A report on the results in dielectrons can be found in [6].

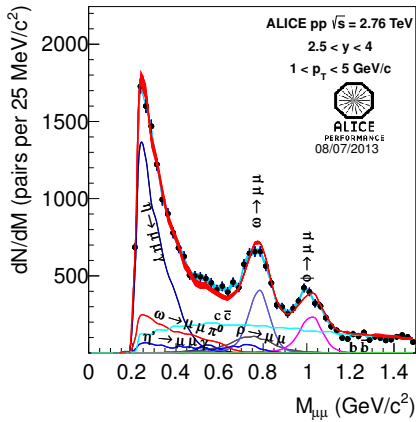
The detector is fully described in [7]. The measurement in the dimuon channel was performed using the forward muon spectrometer, that covers the pseudorapidity range $-4 < \eta < -2.5$ (although in the ALICE reference frame the muon spectrometer covers a negative η range, we chose to present our results in symmetric systems with a positive y notation). It consists of a hadron absorber, a set of cathode pad chambers (five stations, each one composed of two chambers) for the track reconstruction in a dipole magnetic field, an iron wall acting as a muon filter and two stations of two resistive plate chambers for the muon trigger. The centrality is determined with the VZERO detector, that consists of two arrays of plastic scintillators placed at 3.4 m and -0.9 m from the interaction point (IP).

2 Results from pp collisions

Data for pp collisions were taken in 2013 at $\sqrt{s_{NN}} = 2.76$ TeV. The analyzed data sample corresponds to an integrated luminosity $L_{int} = 81.1$ nb $^{-1}$. Data relevant for this analysis were acquired with a dimuon trigger that is provided by the coincidence of two single-muon trigger signals. No hardware p_T threshold is imposed by the trigger. The muon transverse momentum could therefore be measured down to a minimum value of ~ 0.5 GeV/ c , imposed by the presence of the hadron absorber and the muon filter. Offline selections were applied in order to remove beam-gas background. Muon tracks were selected asking that the tracks reconstructed in the tracking stations matched the ones in the trigger chambers and that their pseudorapidity was in the range $-4 < \eta_\mu < -2.5$. Muon pairs were selected requiring that the dimuon rapidity was within the interval $2.5 < y_{\mu\mu} < 4$.

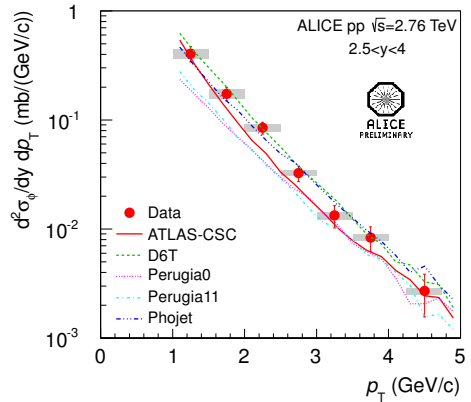
The combinatorial background in the opposite sign dimuon mass spectrum was subtracted using the event mixing technique. The signal to background ratio at the ϕ peak is $S/B \sim 2$.

The mass spectrum after background subtraction, shown in Fig. 1 for dimuon $p_T > 1$ GeV/ c , was described as a superposition of light meson decays into muon pairs, with an additional contribution coming from charm and beauty semi-muonic decays. Low-mass resonance shapes, as well as the acceptance and efficiency for each process, were obtained through a Monte Carlo simulation with a parametric generator [8], while open charm and beauty were generated using a parametrization of PYTHIA. Alternative fits to the mass spectrum were performed replacing this hadronic cocktail with



ALI-PERF-51032

Figure 1. Dimuon invariant mass spectrum for pp collisions at $\sqrt{s} = 2.76$ TeV after combinatorial background subtraction for $1 < p_T < 5$ GeV/c (full circles). Light blue band: systematic uncertainty from background subtraction. Red band: sum of all simulated contributions. The width of the red band represents the uncertainty on the relative normalization of the sources.



ALI-DER-51622

Figure 2. ϕ differential cross section vs p_T for pp collisions at $\sqrt{s} = 2.76$ TeV compared with the predictions based on several PYTHIA tunes and PHOJET. Grey boxes represent the systematic uncertainty.

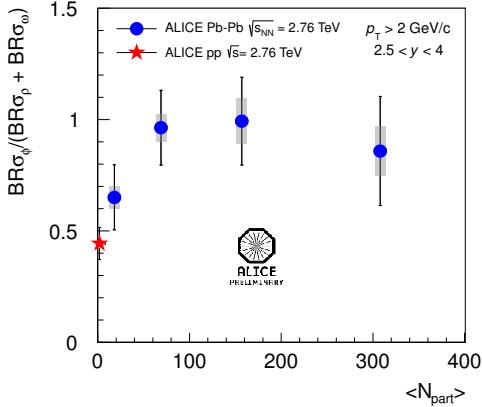
empirical functions. The ϕ p_T -differential cross section was determined as:

$$\frac{d\sigma_\phi}{dy dp_T} = \frac{N_\phi^{\text{meas}}(\Delta p_T)}{A \varepsilon(\Delta p_T) BR_{\phi \rightarrow l^+ l^-} L_{\text{int}}}, \quad (1)$$

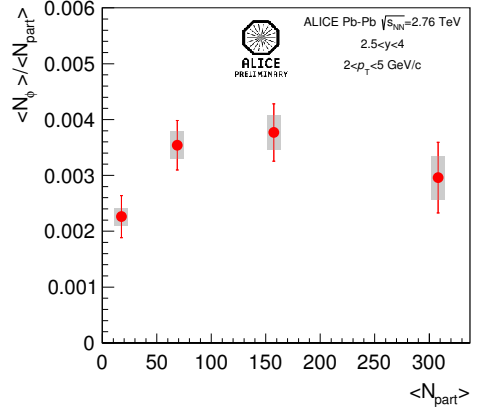
where $N_\phi^{\text{meas}}(\Delta p_T)$ is the raw number of ϕ mesons in a given p_T bin, determined through a fit to the mass spectrum, $BR_{\phi \rightarrow l^+ l^-}$ is the branching ratio for the ϕ decay into lepton pairs (assuming lepton universality, the more precise measurement in $e^+ e^-$ is used), A is the acceptance and ε is the efficiency for the $\phi \rightarrow \mu^+ \mu^-$ process. The sources of systematic uncertainty are those on the evaluation of the branching ratio (1%), on the integrated luminosity (1.8%), on the number of ϕ mesons determined by the fit (ranging from 8.7% at low p_T to 4.6% at high p_T), on the tracking and trigger efficiency (4.5% and 3%, respectively). The differential cross section is reported in Fig. 2. In the same figure, the predictions based on the PYTHIA tunes ATLAS-CSC, D6T, Perugia-0 and Perugia-11 and on PHOJET are shown [9–13]. It can be observed that, while the Perugia-0 and Perugia-11 tunes underestimate the cross section by about a factor of two, the other calculations agree with the measurement within 15%. The considerations on the comparison with the models also hold for the previously analyzed data at $\sqrt{s} = 7$ TeV [8].

3 Results from Pb–Pb collisions

Data for Pb–Pb collisions were collected in 2011 at $\sqrt{s_{\text{NN}}} = 2.76$ TeV. For this data set, a higher p_T selection, with a threshold at about 1 GeV/c, was applied on the single muons at the trigger level. The offline selections applied were the same as in the pp analysis, with an additional cut on the single muon p_T at 0.85 GeV/c that removes muons that, due to the fact that the trigger threshold is not sharp,



ALI-PREL-43838



ALI-PREL-51101

Figure 3. Ratio $BR_{\phi}\sigma_{\phi}/(BR_{\rho}\sigma_{\rho} + BR_{\omega}\sigma_{\omega})$ as a function of the number of participating nucleons $\langle N_{\text{part}} \rangle$. Grey boxes represent the systematic uncertainty.

Figure 4. ϕ multiplicity per participant as a function of the number of participating nucleons. Grey boxes represent the systematic uncertainty.

have been accepted at the trigger level. Due to the limited acceptance at low p_T caused by the high p_T threshold imposed by the trigger, an additional cut on the dimuon p_T at 2 GeV/c was applied.

The combinatorial background was evaluated with the event mixing technique. The S/B ratio at the ϕ peak is about 0.1 for most central collisions, increasing up to 3 for peripheral collisions.

The detector acceptance and efficiency was estimated by means of an embedding Monte Carlo technique. The Monte Carlo hits of muons from ϕ decays were embedded into minimum bias events at the raw-data level. The standard reconstruction algorithm was then applied to these events. This technique allows to account for the variation of the reconstruction efficiency with the detector occupancy and, thus, the collision centrality.

In Fig. 3, the ratio $BR_{\phi}\sigma_{\phi}/(BR_{\rho}\sigma_{\rho} + BR_{\omega}\sigma_{\omega})$, is shown as a function of the number of participating nucleons $\langle N_{\text{part}} \rangle$. The pp result is also reported for comparison. Systematic uncertainties are mainly due to the variations related to the p_T cut applied to the single muons and to the description of the correlated background due to non-resonant components. Other components, like the uncertainty on the tracking and trigger efficiency and on the acceptance, mainly cancel out in the ratio and are thus neglected. The ratio increases from pp to Pb–Pb and tends to saturate when moving from semiperipheral to central collisions. The value for most central Pb–Pb collisions is about two times the one measured for pp collisions. A similar behaviour is observed in the ϕ multiplicity per participant, plotted in Fig. 4: the multiplicity increases faster than $\langle N_{\text{part}} \rangle$ from peripheral to semiperipheral collisions, and tends to saturate for higher $\langle N_{\text{part}} \rangle$ values.

The nuclear modification factor for a given centrality, p_T and y range is obtained as:

$$R_{AA} = \frac{\langle \phi \rangle}{\sigma_{pp} \langle T_{AA} \rangle}, \quad (2)$$

where $\langle \phi \rangle$ is the ϕ multiplicity, σ_{pp} is the cross section for pp collisions in the same p_T and rapidity range and $\langle T_{AA} \rangle$ is the average nuclear overlap function of the considered centrality class [14, 15]. Deviations of R_{AA} from unity quantify the departure of the multiplicity for Pb–Pb from a superposition of incoherent nucleon-nucleon collisions. R_{AA} measured as a function of the number of participants is shown in Fig. 5. In addition to the sources of systematic uncertainties already discussed for the

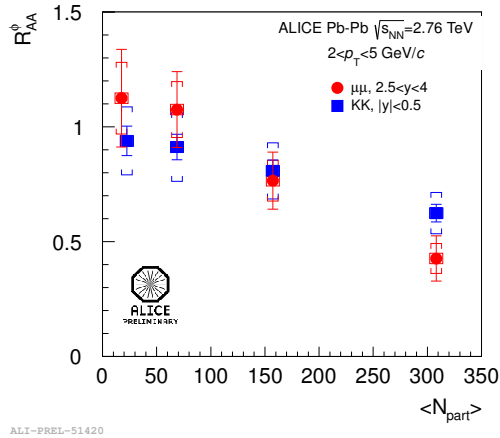


Figure 5. ϕ R_{AA} as a function of $\langle N_{\text{part}} \rangle$ measured in the dimuon channel for $2.5 < y < 4$, compared with the ALICE measurement in the K^+K^- channel for $|y| < 0.5$. Brackets represent the systematic uncertainty.

$BR_{\phi}\sigma_{\phi}/(BR_{\rho}\sigma_{\rho} + BR_{\omega}\sigma_{\omega})$ ratio, also the uncertainty on tracking and trigger efficiency, on the acceptance, on σ_{pp} and $\langle T_{AA} \rangle$ give sizeable contributions to the systematic uncertainty on R_{AA} . In peripheral collisions, the nuclear modification factor is compatible, within uncertainty, with unity, indicating that these collisions behave as a superposition of incoherent pp collisions. In most central collisions, R_{AA} is reduced to about 0.4, showing a clear suppression of the ϕ multiplicity with respect to the pp reference in the intermediate p_T region. The comparison with the results obtained at midrapidity in the KK decay channel shows a point-by-point agreement within the uncertainties. However, the most peripheral points of the R_{AA} at forward rapidity are higher than the ones at midrapidity, while the semicentral and the central points are lower, hinting at two different behaviours: this issue is currently under investigation and may be due to a different hydrodynamic push that the particles are subjected to at forward and at midrapidity in the intermediate p_T region.

4 Results from p–Pb collisions

Data for p–Pb collisions were taken by the ALICE experiment in 2013, at $\sqrt{s_{NN}} = 5.02$ TeV. Due to the different energies of the LHC proton and lead beams ($E_p = 4$ TeV, $E_{Pb} = 1.58$ A·TeV), the nucleon-nucleon center-of-mass in p–Pb collisions moves in the laboratory with a rapidity $y_0 = 0.465$ in the direction of the proton beam. Two beam configurations have been considered for the data taking in p–Pb collisions by inverting the direction of the orbits of the two particle species. This allowed the ALICE muon spectrometer to access two different rapidity regions: $2.03 < y_{cms} < 3.53$, when the proton beam is directed towards the muon spectrometer (proton fragmentation region) and $-4.46 < y_{cms} < -2.96$, when the Pb beam is directed towards the muon spectrometer (Pb nucleus fragmentation region). In the following, these two rapidity ranges will be referred to as "forward" and "backward", respectively.

Events retained for the analysis were selected by means of a dedicated dimuon trigger with no p_T threshold, as for the pp data sample. The analysis of the p–Pb data shares the same strategy described for the pp data: after subtraction of the combinatorial background, estimated by means of an event mixing technique, the invariant mass spectrum of the signal is described in terms of the expected

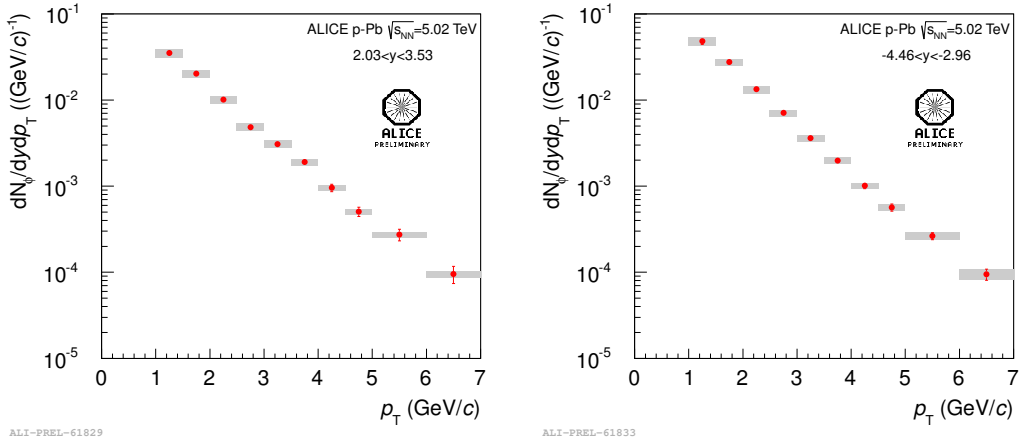


Figure 6. ϕ yield as a function of dimuon p_T for p–Pb collisions at $\sqrt{s_{NN}} = 5.02$ TeV at forward (left) and backward (right) rapidity. Grey boxes represent the systematic uncertainty.

sources. The S/B ratio at the ϕ peak is about 0.7 at forward rapidity and 0.4 at backward rapidity. The yield as a function of p_T for p–Pb collisions was extracted separately for the forward and backward rapidity regions, as shown in Fig. 6. The yield at backward rapidity is higher than the one at forward rapidity, showing an asymmetry in the ϕ production in the proton and lead fragmentation regions.

In order to directly compare the observed yields at forward and backward rapidity, the ϕ yield was also extracted as a function of p_T in the common y_{cms} ranges $-3.53 < y_{cms} < -2.96$ and $2.96 < y_{cms} < 3.53$. The forward/backward ratio for the ϕ yield was found to be ~ 0.5 , with no significant dependence on p_T .

In order to calculate the nuclear modification factor, the pp cross section at $\sqrt{s_{NN}} = 5.02$ TeV is needed. Since no measurement is available at this energy, it was obtained interpolating the results at 2.76 and 7 TeV. For each p_T interval, the differential cross section $d\sigma_{pp}/dydp_T$ at 5.02 TeV was interpolated following the assumption that the cross section increases with \sqrt{s} according to a power law $\sqrt{s} = A \cdot s^n$, where A and n are determined using the data at 2.76 and 7 TeV [8]. The interpolated cross section, which refers to the rapidity range of $-4.0 < y_{cms} < -2.5$, was finally scaled to the forward and backward rapidity windows $2.03 < y_{cms} < 3.53$ and $-4.46 < y_{cms} < -2.96$ as used for the analysis of the p–Pb data. The relative scaling factors were evaluated as an average from simulations with PHOJET and PYTHIA.

The R_{pPb} of the ϕ meson is shown in Fig. 7 as a function of p_T , for the forward and backward rapidity regions. A rising trend of R_{pPb} moving from $p_T = 1$ GeV/c to 3 – 4 GeV/c can be observed both at forward and backward rapidity. The values of R_{pPb} in the two rapidity ranges, however, are significantly different. In particular, at backward rapidity we observe an enhancement of the ϕ cross section with respect to the pp reference, around $p_T = 3 - 4$ GeV/c. This enhancement could be associated either to an initial state effect (including a possible Cronin-like peak [17]) or to a final state effect related to radial flow in p–Pb as proposed for recent ALICE measurements at mid-rapidity [18]. Such an enhancement, reaching a factor of up to 1.6, is a specific feature of the Pb nucleus fragmentation region. As for the trend towards high p_T , we observe that the ϕ meson R_{pPb} presented here is compatible with unity for $p_T > 4$ GeV/c in the proton fragmentation region, similarly to what is observed for the measurement of the charged particle production at mid-rapidity [19]. The observations in the

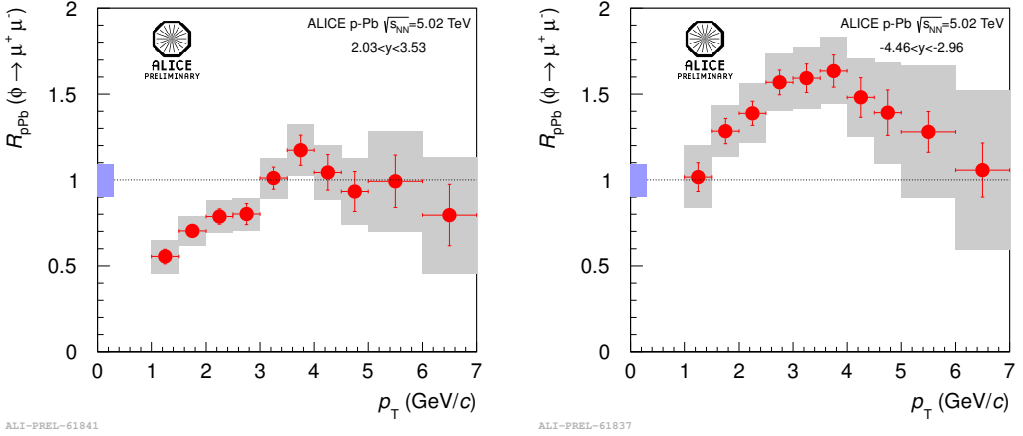


Figure 7. ϕ nuclear modification factor R_{pPb} for p–Pb collisions at forward (left) and backward (right) rapidity. Grey boxes represent the systematic uncertainty.

Pb nucleus fragmentation region do not allow to establish a clear trend of the R_{pPb} factor at high p_T , due to the limited p_T region accessible in the analysis: it should be noticed, however, that a possible saturation to $R_{pPb} \sim 1$ for $p_T > 7$ GeV/c would still be compatible with the available data points.

5 Conclusions

In conclusion, the ϕ production cross section was measured for pp collisions at $\sqrt{s} = 2.76$ TeV. The comparison with some commonly used PYTHIA tunes and PHOJET shows the ATLAS-CSC and D6T tunes, as well as PHOJET, reproduce the measured cross section within $\sim 15\%$, while Perugia-0 and Perugia-11 underestimate the cross section by about a factor of two. The comparison with the models shows similar results as the ones obtained in a previous measurement at $\sqrt{s} = 7$ TeV. For Pb–Pb collisions, the ϕ multiplicity per participant increases from peripheral to semiperipheral collisions and tends to saturate in semicentral and central collisions. The nuclear modification factor is compatible with unity for peripheral collisions and decreases down to ~ 0.5 for most central collisions. The comparison between the ϕ R_{AA} measured in the dimuon decay channel at forward rapidity and in the KK decay channel at midrapidity suggests a different behaviour, probably due to a different hydrodynamic push in the two rapidity domains in the intermediate p_T region $2 < p_T < 5$ GeV/c. The p_T -differential yield of the ϕ meson was measured for p–Pb collisions separately for the forward and backward regions. The forward-backward asymmetry in the ϕ yield was found to be ~ 0.5 , with no significant p_T dependence. The nuclear modification factor R_{pPb} was measured as a function of p_T . In the forward region a rising trend from $R_{pPb} \sim 0.5$ for $p_T = 1$ GeV/c to $R_{pPb} \sim 1$ for $p_T = 4$ GeV/c is observed. In the Pb nucleus fragmentation region, on the other hand, an enhancement is observed for R_{pPb} , reaching values as large as 1.6 around $p_T = 3 - 4$ GeV/c.

References

- [1] P. Braun-Munzinger *et al.*, Invited review for *Quark-Gluon Plasma* Vol. 3 (Singapore: World Scientific) (2003)

- [2] P. F. Kolb and U. W. Heinz, Invited review for *Quark-Gluon Plasma* Vol. 3 (Singapore: World Scientific) (2003)
- [3] D. d'Enterria, Jet Quenching *Preprint* arXiv:0902.2011 [nucl-ex] (2009)
- [4] A. Adare *et al.* (PHENIX Collaboration), *Phys. Rev. C* **83**, 024909 (2011)
- [5] S. Pal *et al.*, *Nucl. Phys. A* **707**, 525 (2002)
- [6] M. K. Kohler *et al.* (ALICE Collaboration), *Preprint* arXiv:1407.7809 (2014)
- [7] K. Aamodt *et al.* (ALICE Collaboration), *JINST* **3**, S08002 (2008)
- [8] B. Abelev *et al.* (ALICE Collaboration), *Phys. Lett. B* **710**, 557 (2012)
- [9] T. Sjöstrand *et al.*, *J. High Energy Phys.* **05**, 026 (2006)
- [10] C. Buttar *et al.*, *Acta Phys. Pol. B* **35**, 433 (2004)
- [11] R. Field, *Acta Phys. Pol. B* **39**, 2611 (2008)
- [12] P. Z. Skands, *Phys.Rev. D* **82**, 074018 (2010)
- [13] R. Z. Engel, *Phys. C* **66**, 203 (1995); R. Engel and J. Ranft, *Phys. Rev D* **54**, 4244 (1996)
- [14] B. Abelev *et al.* (ALICE Collaboration), *Phys. Rev. C* **88**, 044909 (2013)
- [15] A. Toia, *J. Phys. G* **38**, 124007 (2011)
- [16] A. G. Knospe (ALICE Collaboration), *J.Phys.Conf.Ser.* **509**, 012087 (2014)
- [17] A. Accardi, arXiv:hep-ph/0212148 (2002)
- [18] B. Abelev *et al.* (ALICE Collaboration), *Phys.Lett. B* **728**, 25 (2014)
- [19] B. Abelev *et al.* (ALICE Collaboration), *Phys.Rev.Lett.* **110**, 082302 (2013)